

Lepton-flavour universality tests with semi-leptonic B decays at LHCb

Benedetto Gianluca Siddi on behalf of LHCb collaboration¹

Dipartimento di Fisica

Università degli studi di Ferrara

42122 Ferrara, ITALY

CERN, CH-1211 Geneva 23, SWITZERLAND

1 Introduction

Lepton universality, a symmetry of the Standard Model (SM), predicts equal coupling between gauge bosons and the three lepton families. Standard Model extensions give additional interactions, implying in some cases a stronger coupling with the third generation of leptons. Semileptonic decays of b hadrons (hadrons containing a b quark) provide a sensitive probe to such new physics effects. The presence of additional charged Higgs bosons or leptoquarks [1, 2], required by such SM extensions, can have significant effect on the semileptonic decay rate of $B^0 \rightarrow D^{*-}\tau^+\nu_\tau$. Since uncertainties due to hadronic effects cancel to a large extent, the SM prediction for the ratios between branching fractions of semitauponic decays of B mesons relative to decays involving lighter lepton families, such as $R(D^{*+}) = \frac{\mathcal{B}(\bar{B}^0 \rightarrow D^{*+}\tau^-\bar{\nu}_\tau)}{\mathcal{B}(\bar{B}^0 \rightarrow D^{*+}\mu^-\bar{\nu}_\mu)}$ and $R(D^+) = \frac{\mathcal{B}(\bar{B}^0 \rightarrow D^+\tau^-\bar{\nu}_\tau)}{\mathcal{B}(\bar{B}^0 \rightarrow D^+\mu^-\bar{\nu}_\mu)}$, are known with an uncertainty at the percent level [3, 4]. The combination of experimental measurements performed by BaBar[5, 6], Belle [7, 8] and LHCb [9] observing the channel where the τ decays in leptons or in one prong particle [10], gives a deviation from the SM prediction of about 4σ . It is therefore important to perform additional measurements in this sector in order to improve the precision and confirm or disprove this deviation. Another possibility is to perform these measurements using $\tau^- \rightarrow \pi^-\pi^+\pi^-\nu_\tau$ decay channel (3-prong decay). A measurement of $R(D^{*-})$ using 3-prong τ decays performed by LHCb is reported. This report, references the article [11], submitted to arXiv.

2 Semitauponic decays of b hadrons

Semitauponic decays of B^0 and B^+ mesons are successfully studied in *B-factories* with high-statistics samples. Despite the hadronic environment, LHCb is also able

¹Talk presented at the APS Division of Particles and Fields Meeting (DPF 2017), July 31-August 4, 2017, Fermilab. C170731

to study such kind of decays and extend to other b hadrons (B_s^0 , Λ_b^0 , B_c^+) thanks to the high boost and the excellent vertexing capabilities. However, there are some analysis challenges in a hadronic environment. Rest frame variables are needed in order to distinguish between signal and background. Backgrounds due to unreconstructed charged and neutral particles must be suppressed. A normalization channel, necessary to reduce at minimum systematic uncertainties, must be identified.

A way to measure $R(D^{*-})$ is to reconstruct the τ in the 3-pions decay channel. This is a semileptonic decay without charged leptons in the final state. In this case, the measured quantity is:

$$K(D^{*-}) = \frac{\mathcal{B}(B^0 \rightarrow D^{*-}\tau^+\nu_\tau)}{\mathcal{B}(B^0 \rightarrow D^{*-}\pi^+\pi^-\pi^+)} = \frac{N_{sig}}{N_{norm}} \frac{\epsilon_{norm}}{\epsilon_{sig}} \frac{1}{\mathcal{B}(\tau^+ \rightarrow 3\pi(\pi^0)\bar{\nu}_\tau)} \quad (1)$$

where N_{sig} and N_{norm} are the signal and the normalization yields, ϵ_{sig} and ϵ_{norm} are the efficiencies for the signal and normalization decay modes, respectively.

The two decays modes share the same visible final state and most of the systematic uncertainties will cancel. Then, $R(D^{*-})$ can be measured using:

$$R(D^{*-}) = K(D^{*-}) \times \frac{\mathcal{B}(B^0 \rightarrow D^{*-}3\pi)}{\mathcal{B}(B^0 \rightarrow D^{*-}\mu^+\nu_\mu)} \quad (2)$$

The quantities multiplying $K(D^{*-})$ are taken as external inputs [12].

3 Events selection and main backgrounds

3.1 Detached-vertex method

The most abundant background source is due to hadronic B decays into $D^{*-}3\pi X$, where X denotes unreconstructed particles. Such background has a branching fraction that is about 100 times that of the signal.

$$\frac{\mathcal{B}(B^0 \rightarrow D^{*-}3\pi X)}{\mathcal{B}(B^0 \rightarrow D^{*-}\tau^+\nu)_{SM}} \sim 100$$

In Fig. 1 a schematic view of the $B^0 \rightarrow D^{*-}3\pi X$ decay is shown.

In the signal case, because of the significant τ lifetime and boost along the forward direction, the 3π system is detached from the B^0 vertex. Thanks to the excellent vertex resolution, it is possible to require a detached vertex topology for the τ particle. This consists on the requirement that the τ vertex is downstream with respect to the B^0 vertex along the beam direction (Δ_z) with a significance of at least 4σ . A schematic view of this requirement is shown in Fig. 2. Using this requirement, the background due to $B \rightarrow D^{*-}3\pi X$ is suppressed by about 3 orders of magnitude.

The distribution of the quantity $\Delta_z/\sigma_{\Delta_z}$ for different background sources is presented in Fig. 3. The contribution from $B \rightarrow D^{*-}3\pi X$ decays (grey) is suppressed, after a cut of $\Delta_z/\sigma_{\Delta_z} > 4$.

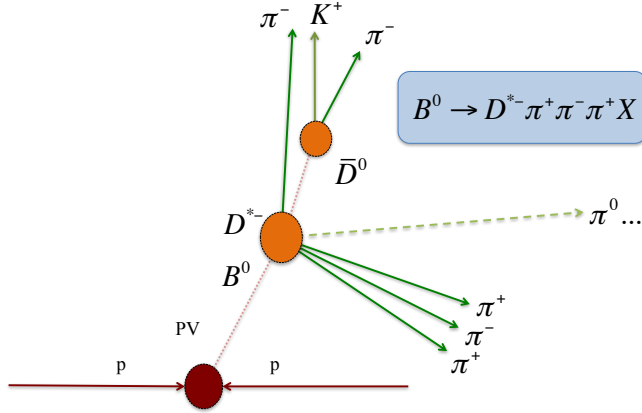


Figure 1: Schematic view of the $B^0 \rightarrow D^{*-} 3\pi X$ decay in which the 3-pions comes from the B^0 vertex.

3.2 Double charm decays

After the detached-vertex requirement, the remaining background consists of B hadron decays where the 3π vertex is transported away from the B vertex by a charm carrier, such as D^0 , D^+ and D_s^+ mesons. This background has a yield that is about 10 times the signal.

$$\frac{\mathcal{B}(B^0 \rightarrow D^* D_{(s)}^{(*)}; D_{(s)}^{(*)} \rightarrow 3\pi + X)}{\mathcal{B}(B^0 \rightarrow D^* \tau \nu)} \sim 10$$

To suppress these background sources, LHCb has three very good tools: the 3π dynamics;

- the isolation criteria against charged tracks and neutral energy deposits;
- partial reconstruction techniques in the signal and background hypotheses.

All these variables are used to train a boosted decision tree (BDT), where $B^0 \rightarrow D^{*-} \tau^+ \nu_\tau$ simulation is used as signal, and double charm simulated decays, $B \rightarrow D^* D X$, as background. The output of the BDT is shown in Fig. 4.

3.3 A model for $D_s^+ \rightarrow 3\pi X$ decays

The dominant double-charm background process $B \rightarrow D^{*-} D_s^+(X)$ is reduced by taking into account the resonant structure of the 3π system. The τ lepton decays to $3\pi \nu_\tau$

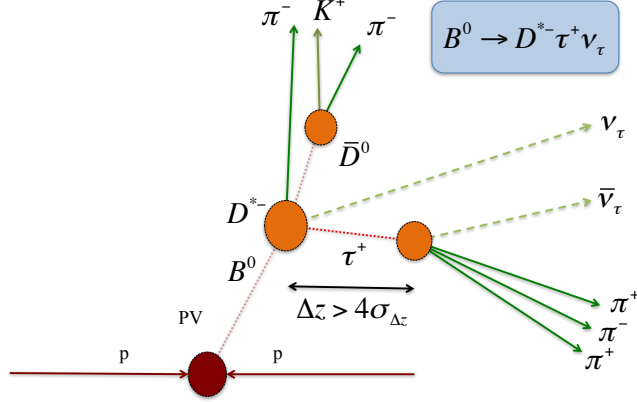


Figure 2: Schematic view of the detached-vertex requirement.

final states predominantly through the $a_1(1260)^+ \rightarrow \rho^0 \pi^+$ decay. By contrast, the D_s^+ meson decays to $3\pi X$ final states predominantly through the η and η' resonances. For this reason, the $D_s^+ \rightarrow 3\pi X$ decay model has been determined directly from data, using a sample formed by events with low value of the BDT output, which is enriched in such decays. In order to retrieve the sub-decays relative fractions, a simultaneous fit to the minimum and maximum of $\pi^+ \pi^-$ mass distribution, the invariant mass of the 2 pions with the same charge the invariant mass of the 3π system has been performed. The fit result is shown in Fig. 5. The model contains the following components:

- D_s^+ decays where at least 1 pion comes from the decay of a η or η' meson : $\eta\pi$, $\eta\rho$, $\eta'\pi$ and $\eta'\rho$;
- D_s^+ decays where at least 1 pion is from an IS (Intermediate Resonance) other than η and η' : $IS\pi$, $IS\rho$ (IS could be ω , ϕ);
- D_s^+ decays where none of the 3 pions comes from an IS, subdivided in: $K^0 3\pi$, $\eta 3\pi$, $\eta' 3\pi$, $\omega 3\pi$, $\phi 3\pi$, 3π non resonant final state.

The results obtained by the fit are then used to construct the D_s^+ template used in the final fit.

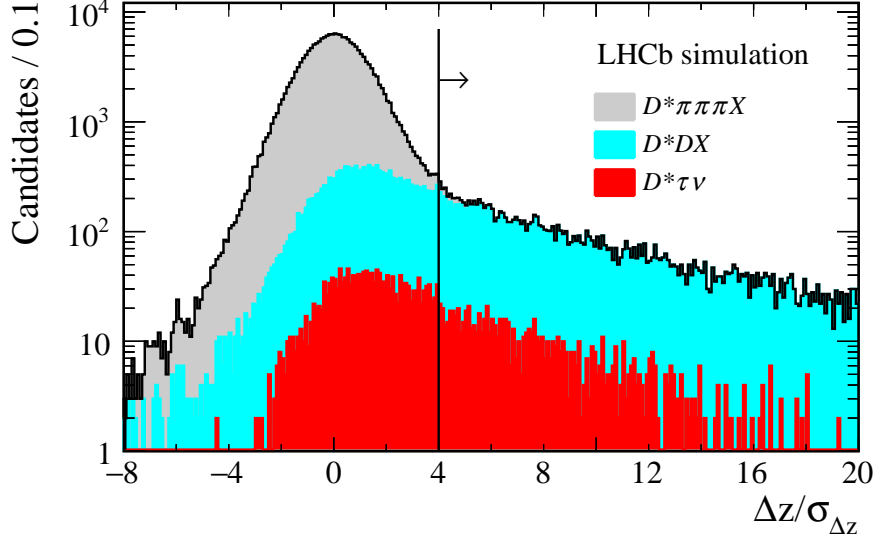


Figure 3: Distribution of the vertex significance (Δ_z/σ) for different background sources.

4 Signal extraction

4.1 Signal reconstruction

Due to the presence of the neutrino in the final state of the signal decay, the τ momentum can be inferred, up to a two-fold ambiguity, by exploiting the flight direction of the τ . In this way it is possible to compute the τ momentum with the following equation:

$$|\vec{p}_\tau| = \frac{(m_{3\pi}^2 + m_\tau^2)|\vec{p}_{3\pi}| \cos \theta \pm E_{3\pi} \sqrt{(m_\tau^2 - m_{3\pi}^2)^2 - 4m_\tau^2 |\vec{p}_{3\pi}|^2 \sin^2 \theta}}{2(E_{3\pi}^2 - |\vec{p}_{3\pi}|^2 \cos^2 \theta)} \quad (3)$$

where θ is the angle between τ and 3π direction as shown in Fig. 6.

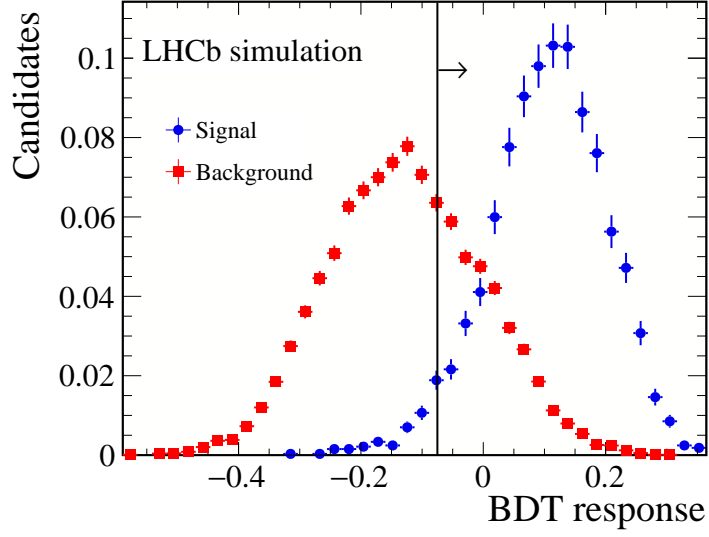


Figure 4: Distribution of the BDT response on the signal and background simulated samples.

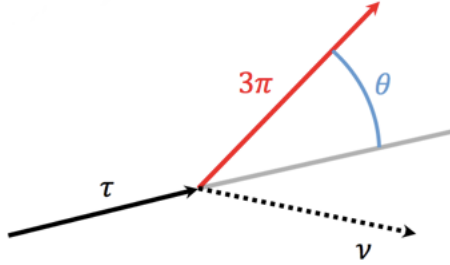


Figure 6: Schematic view of θ , the angle between τ and 3π direction.

The ambiguity can be resolved by choosing the maximum value for the opening angle between the three charged pions system and the direction of the τ lepton, as in the following equation:

$$\theta_{max} = \arcsin\left(\frac{m_{\tau}^2 - m_{3\pi}^2}{2m_{\tau}|\vec{p}_{3\pi}|}\right) \quad (4)$$

This introduces a negligible bias in the signal reconstruction.

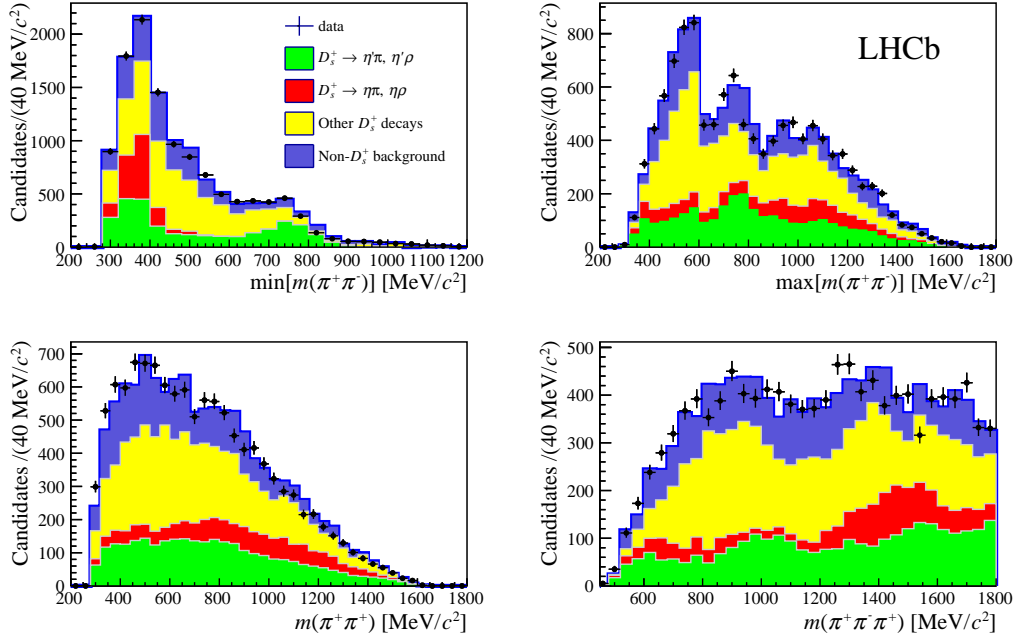


Figure 5: D_s^+ model fit on data. The different contributions are shown.

4.2 Fit model and results

An extended maximum likelihood 3-dimensional fit, using templates has been performed. The fitted variables are:

- q^2 , the invariant mass squared of the $\tau - \nu$ system
- τ decay time;
- The output of the BDT.

The fit model used to extract the signal yield consists of 5 main categories:

- Signal described by the sum of two τ decays, $\tau^+ \rightarrow 3\pi\bar{\nu}_\tau$ and $\tau^+ \rightarrow 3\pi\pi^0\bar{\nu}_\tau$;
- $B \rightarrow D^{**}\tau^+\nu_\tau$ decays;
- $B \rightarrow D^*D_s^+X$, $B \rightarrow D^*D^0X$ and $B \rightarrow D^*D^+X$ decays;
- $B \rightarrow D^{*-}3\pi X$ decays;
- Combinatorial background.

The results of the three-dimensional fit are shown in Fig. 7. A signal yield of $N_{sig} = 1273 \pm 85$ is found, where a 3% correction due to fit bias has been applied. Figure 8 shows the results on the fit in bins of the BDT output.

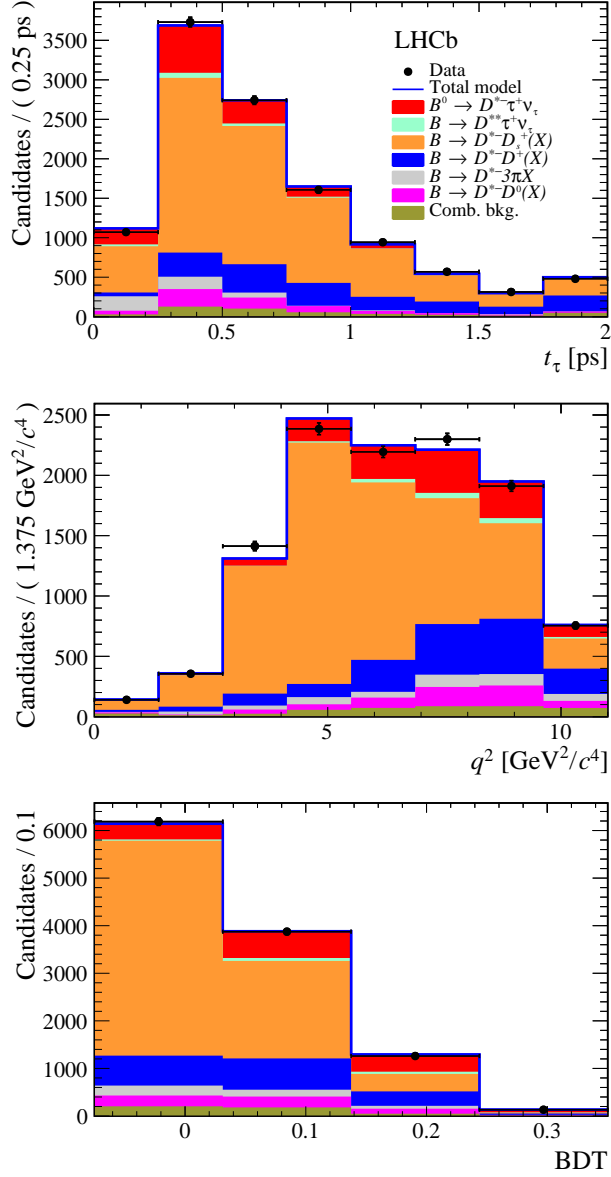


Figure 7: Projections of the three-dimensional fit on the (top) 3π decay time, (middle) q^2 and (bottom) BDT output distributions. The various components are described in the legend.

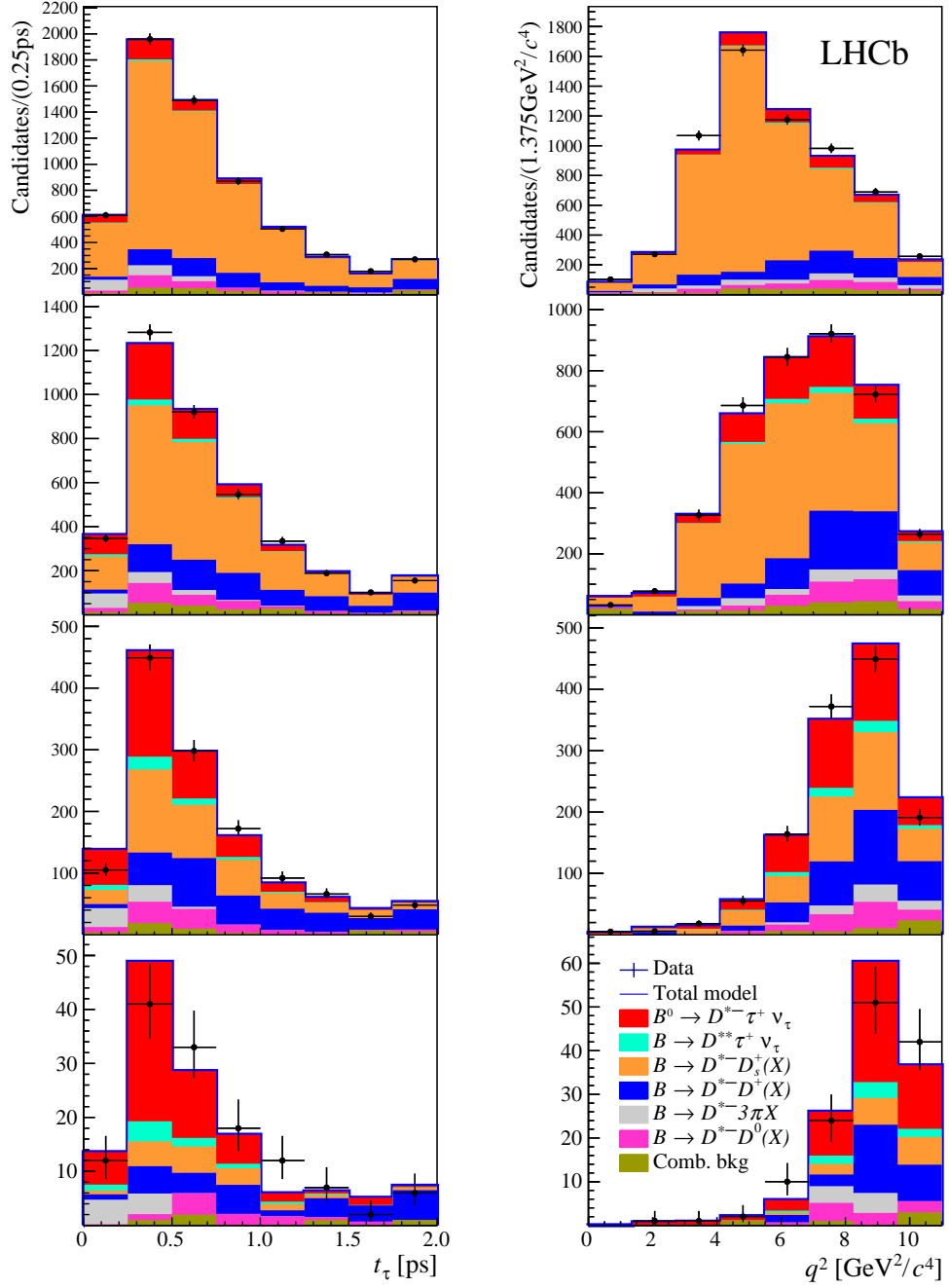


Figure 8: Fit projections on the (left) 3π decay time and (right) q^2 distributions for the four different BDT bins shown in Fig. 7 (bottom). The highest BDT bin corresponds to the two lower figures.

5 Control samples

The fit that determines the signal yield uses templates that are taken from the simulation. It is therefore important to verify the agreement between data and simulation for background processes. Data control samples are used wherever is possible for this purpose. The relative contributions of double-charm backgrounds and their q^2 distribution from simulation are validated, and corrected where appropriate, by using data control samples enriched in such processes. In this way it is also possible to study inclusive decays of D^0 , D^+ and D_s^+ mesons to 3π . In Fig. 9 are shown the data control samples for $D_s^+ \rightarrow \pi^+\pi^-\pi^+$ decays (top left), the $D^0 \rightarrow K^-\pi^+\pi^-\pi^+$ decay (top right) obtained requiring an extra particle in a cone around the 3π flight direction, and the $D^+ \rightarrow K^-\pi^+\pi^+$ decays (bottom) obtained requiring the opposite charged pion to identified as a kaon.

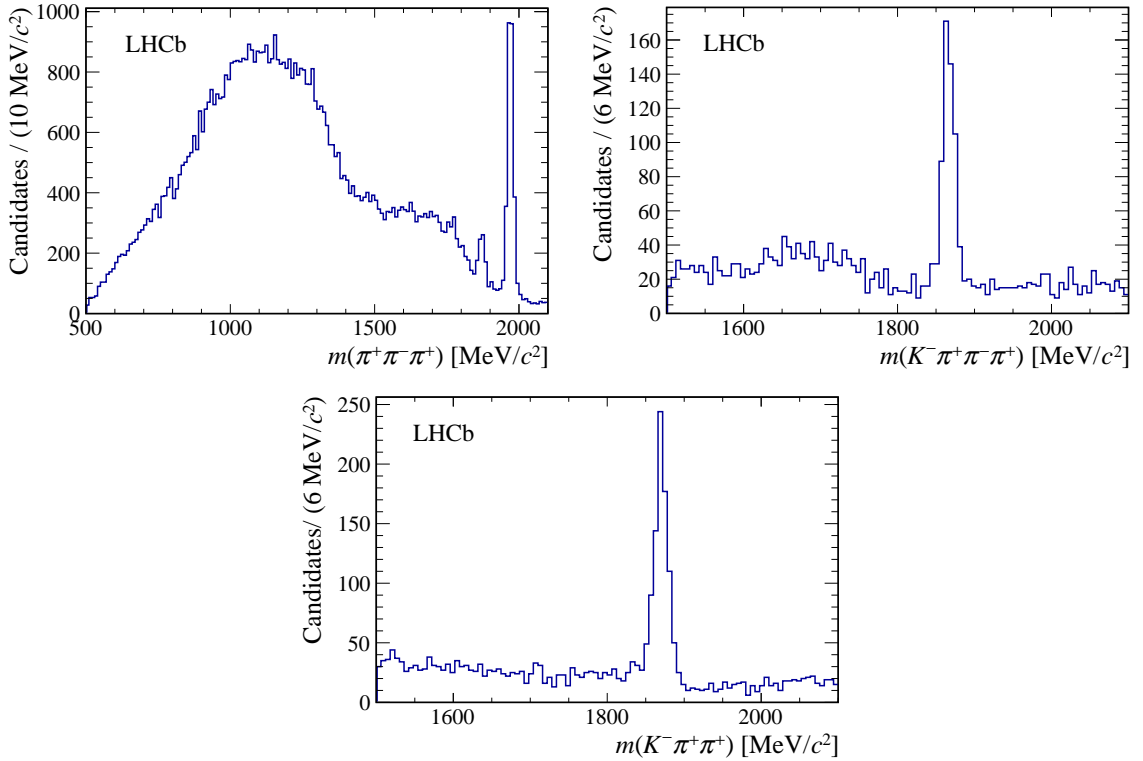


Figure 9: Data control samples for $D_s^+ \rightarrow \pi^+\pi^-\pi^+$ decays (top left), the $D^0 \rightarrow K^-\pi^+\pi^-\pi^+$ decay (top right) obtained requiring an extra particle in a cone around the 3π flight direction, and the $D^+ \rightarrow K^-\pi^+\pi^+$ decays (bottom) obtained requiring the opposite charged pion to identified as a kaon.

6 Normalization mode

The normalization channel has to be as similar as possible to the signal channel in order to cancel all systematics linked to trigger selection, particle identification and selection cuts. The two decays differ by the presence of a softer pion and D^* in the signal decay due to the two extra neutrinos, and the kinematics of the 3π system. This will give a residual effect on the efficiency ratio. Figure 10 shows the $D^{*-}3\pi$ invariant mass after the selection of the normalization sample. A clear B^0 peak signal is seen. In order to extract the normalization yield, a fit is performed in the 5150-5400 MeV/c^2 region. The signal is described by the sum of a Gaussian and a Crystal Ball function. An exponential function is used to describe the background. The yield obtained is $N_{norm} = 17808 \pm 143$.

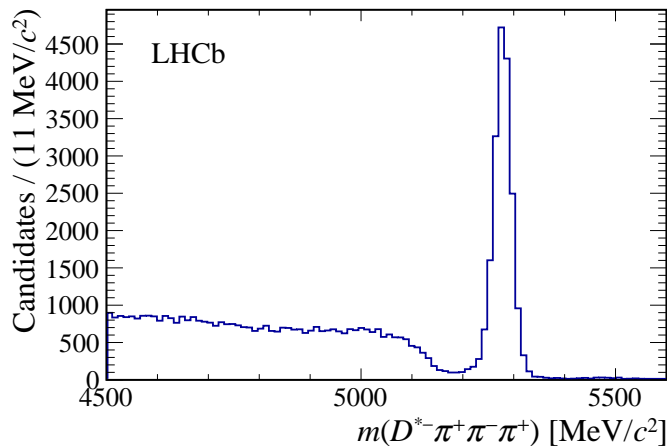


Figure 10: Distribution of the $D^{*-}3\pi$ mass for candidates passing the selection.

7 Systematic uncertainties

Systematic uncertainties on $K(D^{*-})$ are reported in Table 1. The main systematic uncertainties are due to the limited size of the simulated samples that contributes to the efficiencies and to the determination of the template shapes for signal and background. The presence of empty bins in the templates used in the fit introduces a positive bias in the determination of the signal yield that is corrected for. In the uncertainty computation, another contribution is given by the knowledge of the $B \rightarrow D^{*-}(D_s, D^0, D^+)X$ and $B \rightarrow D^{*-}3\pi X$ background shapes. When computing $R(D^{*-})$, an additional systematic of 4.5% due to the knowledge of the external branching fraction must be taken into account. The size of the total systematics is above the statistical precision but there is room for improvements, i.e., with more data

Table 1: Relative systematic uncertainties on $\mathcal{K}(D^{*-})$.

Source	$\delta K(D^{*-})/K(D^{*-})[\%]$
Simulated sample size	4.7
Empty bins in templates	1.3
Signal decay model	1.8
$D^{**}\tau^+\nu_\tau$ and $D_s^{**}\tau^+\nu_\tau$ feeddowns	2.7
$D_s^+ \rightarrow 3\pi X$ decay model	2.5
$B \rightarrow D^{*-}D_s^+X$, $B \rightarrow D^{*-}D^+X$, $B \rightarrow D^{*-}D^0X$ backgrounds	3.9
Combinatorial background	0.7
$B \rightarrow D^{*-}3\pi X$ background	2.8
Efficiency ratio	3.9
Total uncertainty	8.9

and simulated samples, and a better knowledge of the external branching fractions using also results from other experiments.

8 Conclusions

The first measurement of $R(D^{*-})$ with three pions τ decays has been performed, using a technique that is complementary to all previous measurements of this quantity and offer the possibility to study other b-hadron decay modes in a similar way. The ratio of branching fractions between the $B^0 \rightarrow D^{*-}\tau^+\nu_\tau$ and the $B^0 \rightarrow D^{*-}3\pi$ decays is measured to be

$$K(D^{*-}) = 1.93 \pm 0.13 \text{ (stat)} \pm 0.17 \text{ (syst)},$$

where the first uncertainty is statistical and the second systematic. The first determination of $R(D^{*-})$ performed by using 3-pion τ decays is obtained by using the measured branching fractions of $\mathcal{B}(B^0 \rightarrow D^{*-}\mu^+\nu_\mu) = (4.88 \pm 0.10) \times 10^{-2}$ and $\mathcal{B}(B^0 \rightarrow D^{*-}3\pi) = (7.21 \pm 0.29) \times 10^{-3}$, with the result: $R(D^{*-}) = 0.285 \pm 0.019 \text{ (stat)} \pm 0.025 \text{ (syst)} \pm 0.013 \text{ (ext)}$, is one of the most precise single measurement performed so far. It is 1.0 standard deviation higher than the SM prediction 0.252 ± 0.003 , and consistent with previous determinations.

References

- [1] M. Tanaka. Charged higgs effects on exclusive semi-tauonic b decays. *Zeitschrift für Physik C Particles and Fields*, 67(2):321–326, Jun 1995.

- [2] I. Doršner, S. Fajfer, A. Greljo, J.F. Kamenik, and N. Košnik. Physics of leptons in precision experiments and at particle colliders. *Physics Reports*, 641:1 – 68, 2016.
- [3] Dante Bigi and Paolo Gambino. Revisiting $B \rightarrow Dl\nu$. *Phys. Rev.*, D94:094008, 2016.
- [4] Svjetlana Fajfer, Jernej F. Kamenik, and Ivan Nisandzic. On the $B \rightarrow D^*\tau\bar{\nu}_\tau$ sensitivity to new physics. *Phys. Rev.*, D85:094025, 2012.
- [5] J. P. Lees et al. Measurement of an excess of $\bar{B} \rightarrow D^{(*)}\tau^-\bar{\nu}_\tau$ decays and implications for charged Higgs bosons. *Phys. Rev.*, D88:072012, 2013.
- [6] J. P. Lees et al. Evidence for an excess of $\bar{B} \rightarrow D^*\tau^-\bar{\nu}_\tau$ decays. *Phys. Rev. Lett.*, 109:101802, 2012.
- [7] M. Huschle et al. Measurement of the branching ratio of $\bar{B} \rightarrow D^{(*)}\tau^-\bar{\nu}_\tau$ relative to $\bar{B} \rightarrow D^{(*)}l^-\bar{\nu}_l$ decays with hadronic tagging at Belle. *Phys. Rev.*, D92:072014, 2015.
- [8] Y. Sato et al. Measurement of the branching ratio of $\bar{B}^0 \rightarrow D^{*+}\tau^-\bar{\nu}_\tau$ relative to $\bar{B}^0 \rightarrow D^{*+}l^-\bar{\nu}_l$ decays with a semileptonic tagging method. *Phys. Rev.*, D94:072007, 2016.
- [9] Roel Aaij et al. Measurement of the ratio of branching fractions $\mathcal{B}(\bar{B}^0 \rightarrow D^{*+}\tau^-\bar{\nu}_\tau)/\mathcal{B}(\bar{B}^0 \rightarrow D^{*+}\mu^-\bar{\nu}_\mu)$. *Phys. Rev. Lett.*, 115:111803, 2015.
- [10] S. Hirose et al. Measurement of the τ lepton polarization and $r(D^*)$ in the decay $\bar{B} \rightarrow D^*\tau^-\bar{\nu}_\tau$. *Phys. Rev. Lett.*, 118:211801, May 2017.
- [11] Roel Aaij et al. Measurement of the ratio of the $B^0 \rightarrow D^{*-}\tau^+\nu_\tau$ and $B^0 \rightarrow D^{*-}\mu^+\nu_\mu$ branching fractions using three-prong τ -lepton decays. 2017.
- [12] C. Patrignani et al. Review of particle physics. *Chin. Phys.*, C40:100001, 2016. and 2017 update.